Article

FUNCTIONAL CHARACTERIZATION AND IMMUNOLOCALIZATION OF ODORANT BINDING PROTEIN 1 IN THE LUCERNE PLANT BUG, *Adelphocoris lineolatus* (GOEZE)

Shao-Hua Gu
State Key Laboratory for Biology of Plant Diseases and Insect Pests, Institute of Plant Protection, Chinese Academy of Agricultural Sciences, Beijing, China

Wei-Xuan Wang
State Key Laboratory of Agrobiotechnology, College of Biological Sciences, China Agricultural University, Beijing, China

Gui-Rong Wang, Xue-Ying Zhang, and Yu-Yuan Guo
State Key Laboratory for Biology of Plant Diseases and Insect Pests, Institute of Plant Protection, Chinese Academy of Agricultural Sciences, Beijing, China

Ziding Zhang
State Key Laboratory of Agrobiotechnology, College of Biological Sciences, China Agricultural University, Beijing, China

Jing-Jiang Zhou
Department of Biological Chemistry, Rothamsted Research, Harpenden, United Kingdom

Yong-Jun Zhang
State Key Laboratory for Biology of Plant Diseases and Insect Pests, Institute of Plant Protection, Chinese Academy of Agricultural Sciences, Beijing, China

Grant sponsor: National Natural Science Foundation of China; Grant numbers: 31071694; 30871640; Grant sponsor: China National "973" Basic Research Program; Grant number: 2007CB109202; Grant sponsor: State High Technology Development Program; Grant number: 2008AA02Z307.
Shao-Hua Gu and Wei-Xuan Wang contributed equally to this work.
Correspondence to: Yong-Jun Zhang, State Key Laboratory for Biology of Plant Diseases and Insect Pests, Institute of Plant Protection, Chinese Academy of Agricultural Sciences, Beijing 100193, China. E-mail: yjzhang@ippcaas.cn or Jing-Jiang Zhou, Department of Biological Chemistry, Rothamsted Research, Harpenden AL5 2JQ, UK. E-mail: jing-jiang.zhou@bbsrc.ac.uk

ARCHIVES OF INSECT BIOCHEMISTRY AND PHYSIOLOGY, Vol. 77, No. 2, 81–98 (2011)
Published online in Wiley Online Library (wileyonlinelibrary.com).
 DOI: 10.1002/arch.20427

In the insect phylum, the relationships between individuals and their environment are often modulated by chemical communication. Odorant binding proteins (OBPs) are widely and robustly expressed in insect olfactory organs and play a key role in chemosensing and transporting hydrophobic odorants across the sensillum lymph to the olfactory receptor neuron. In this study, a novel OBP gene (AlinOBP1) in the lucerne plant bug, Adelphocoris lineolatus was identified, cloned and expressed. Real-time PCR results indicated that the expression level of AlinOBP1 gene differed in each developmental stage (from first instar to adult) and was predominantly expressed in the antennae of adults. The expression level of AlinOBP1 was 1.91 times higher in male antennae than in female antennae. The binding properties of AlinOBP1 with 114 odorants were measured using a fluorescence probe, N-phenyl-1-naphthylamine (1-NPN), with fluorescence competitive binding. The results revealed that AlinOBP1 exhibits high binding abilities with two major putative pheromone components, ethyl butyrate and trans-2-hexenyl butyrate. In addition, it was observed that six volatiles released from cotton, octanal, nonanal, decanal, 2-ethyl-1-hexanol, β-caryophyllene and β-ionone also bind to AlinOBP1. Immunocytochemistry analysis showed that AlinOBP1 was expressed in the sensillum lymph of sensilla trichodica and sensilla basiconca. Our results demonstrate that AlinOBP1 may function as a carrier in the chemoperception of the lucerne plant bug. © 2011 Wiley Periodicals, Inc.

Keywords: *Adelphocoris lineolatus* (Goeze); odorant binding protein; protein expression; expression pattern; fluorescence binding; molecular model; Immunocytochemistry

INTRODUCTION

Plant bugs (Hemiptera: Miridae) and stink bugs are destructive pests of cotton (Greene et al., 1999; Wu et al., 2002; Lu et al., 2010). Plant bugs like other insects search and locate their hosts relying on highly specific and sensitive olfaction systems to detect specific odorants for food source, oviposition sites, mating with partners and avoidance of toxins and predators (Breer et al., 1994; Field et al., 2000). Exploration of the insect olfactory system could help us to understand the mechanism of the insect olfactory perception processes in searching and locating the hosts and mates, which can further facilitate the design and implementation of novel intervention strategies (Plettner, 2002; Zhou et al., 2010).

In insects, olfactory perception is mediated by proteins located in the sensory hairs of the antennae, including odorant binding proteins (OBPs), chemosensory proteins (CSPs), olfactory receptors (ORs), odorant degrading enzymes (ODEs) and sensory neuron membrane proteins (SNMPs) (Vogt and Riddiford, 1981; Vogt et al., 1985; Wanner et al., 2004; Vogt et al., 2009; Zhou, 2010). Among these proteins, OBPs are the most abundant and expected to be involved in the first biochemical step in odorant reception. Insect OBP family can be divided into three major classes, pheromone binding proteins (PBPs) (Vogt and Riddiford, 1981), general odorant binding proteins (GOBP1 and GOBP2) (Vogt et al., 1991), and antennal binding proteins X (ABPX)

(Krieger et al., 1996). So far, OBPs have been identified in many insect orders such as in Lepidoptera (Vogt and Riddiford, 1981), Orthoptera (Ban et al., 2003), Isoptera (Krieger and Ross, 2002), Diptera (Xu et al., 2003), Hymenoptera (Zhang et al., 2009), Hemiptera (Dickens et al., 1995) and Coleoptera (Graham et al., 2003).

There are several proposed functions of OBPs in odor and pheromone perception, including (i) transporting odorants or pheromones across the sensillum lymphs to the ORs, which can activate signal transduction process (Krieger and Breer, 1999); (ii) solubilizing hydrophobic odorants (Steinbrecht, 1998); (iii) concentrating odorants in the sensillum lymph (Steinbrecht, 1998); (iv) removing or deactivating odorants after stimulating the receptors (Vogt and Riddiford, 1981; Ziegelberger, 1995). However, the experimental data which support those supposed functions are exclusive.

The key function of OBPs is their ability to bind semiochemicals and measured mainly by fluorescence displacement binding assay (Pelosi et al., 2006; Zhou, 2010). The most widely used fluorescent probe is *N*-phenyl-1-naphthylamine (1-NPN), which has been employed in the binding of *Drosophila* LUSH (Zhou et al., 2004), the *Locusta migratoris* LmigOBP1-3 (Jiang et al., 2009; Yu et al., 2009), the social wasp *Polistes dominulus* OBP1 (Calvello et al., 2003) and *Bombyx mori* OBPs (Zhou et al., 2009; He et al., 2010).

In this study, a novel OBP gene (*AlinOBP1*) in the antennae of the lucerne plant bug, *Adelphocoris lineolatus* (Goeze) was identified, cloned and expressed. The binding properties of the recombinant protein AlinOBP1 with 114 odorants were characterized by fluorescence competitive binding method. In addition, the tissue location of AlinOBP1 in different sensilla was investigated by immunocytochemistry method.

MATERIALS AND METHODS

Real-Time Quantitative PCR

A. lineolatus nymphs and adults were collected from cotton fields at the Langfang Experimental Station of Chinese Academy of Agricultural Sciences, Hebei Province, China. Male antennae, female antennae, heads (without antennae), thoraxes, abdomens, legs and wings of adult individuals were excised and immediately frozen in liquid nitrogen.

Total RNA was isolated using Trizol reagent (Invitrogen, Carlsbad, CA) and then treated with DNase I (Invitrogen, Carlsbad, CA) to remove residual genomic DNA. cDNA was synthesized by using SuperScript^{TM} III Reverse Transcriptase system (Invitrogen, Carlsbad, CA).

Real-time PCR was performed on 7500 Fast Detection System (Applied Biosystems, Carlsbad, CA). Taqman primers and probes were designed using Primer Express 3.0 (Applied Biosystems, Carlsbad, CA) (Table 1). Detailed protocols for qPCR have been described previously (Gu et al., 2011).

The sequence of *AlinOBP1* (GenBank No. GQ477022) was obtained from the antennal cDNA library of *A. lineolatus* by EST sequencing and BLASTX. As an endogenous control, the *A. lineolatus* β-actin gene (GenBank No.GQ477013) was used to normalize the target gene expression and correct for sample-to-sample variation. qPCR cycling parameters are: 95°C, 10 s, 40 cycles at 95°C for 20 s, 60°C for 34 s. To check reproducibility, test samples, endogenous control and negative control were

Table 1. Primers Used for Clone and Expression Analysis of AlinOBP1

Primer name	*Sequence (5′-3′)*	*Position (bp)*	*Product size*
cDNA Isolation			
OBP1-Forward	GCGGATCCATGAACTCACTCATTCCCGT	85–104	438 bp
OBP1-Reverse	GCGCTCGAGTTAGAAGTCTGGAGGACGC	504–522	
Real-time PCR			
OBP1-Forward	GAGGGCAGACGAACAAACCA	132–151	60 bp
OBP1-Reverse	TCCTCCCGGCATTTGTTG	174–191	
OBP1-Probe	FAM-CGCCATGGTAGCCAAAGCCT-TAMRA	153–172	
β-*actin*-Forward	CTCTGGAGGCACCACCATGTA	60–80	68 bp
β-*actin*-Reverse	GGGCAAGAGCGGTGATTTC	109–127	
β-*actin*-Probe	FAM-CCCGGAATCGCTGACAGGATGC-TAMR	82–103	

done in triplicate with two biological samples. *AlinOBP1* gene expression levels in each tissue and developmental stage was calculated using the comparative $2^{-\Delta\Delta CT}$ method (Livak and Schmittgen, 2001).

Expression and Purification of AlinOBP1

Full-length cDNA encoding AlinOBP1 was amplified by RT-PCR with gene specific primers (Table 1). The RT-PCR product was first cloned into pGEM-T easy vector (Promega, Madison, WI) and then subcloned into the bacterial expression vector pET30a (+) (Novagen, Madison, WI) between the *Bam*H I and *Xho*I restriction sites. The plasmid containing the correct AlinOBP1 sequence was then extracted and transformed into *E.coli* BL21(DE3) competent cells. Single colony was grown overnight in 50 ml LB broth (including 100 μg/ml kanamycin). Five liters of LB medium was inoculated with the 50 ml overnight culture at 37°C for 2–3 h until the absorbance at OD_{600} reached 0.6. The protein expression was then induced for 8 h using IPTG with a final concentration of 1 mM at 28°C. The bacterial cells were harvested by centrifugation (8,000 *g*, 10 min), resuspended in a lysis buffer (80 mM Tris-HCl, 200 mM NaCl, 1 mM EDTA, 4% glycerol, PH 7.2, 0.5 mM PMSF), lysed by sonication (10 s, 5 passes) and centrifuged again (12,000 *g*, 10 min). The supernatant were collected and purified by HisTrap affinity columns (GE Healthcare Biosciences, Uppsala, Sweden) and then desalted by HiTrap Desalting Columns (GE Healthcare Biosciences, Uppsala, Sweden). Soon after the protein was concentrated and the his-tag was removed by recombinant enterokinase (rEK) (Novagen, Madison, WI), followed by a second purification on the HisTrap affinity columns and desalination on the HiTrap Desalting Columns. The size and purity of AlinOBP1 were checked by sodium dodecyl sulfate polyacrylamide gel electrophoresis (SDS-PAGE).

Preparation of Antisera

Antisera were obtained by injecting an adult male rabbit subcutaneously and intramuscularly. The protein was emulsified with an equal volume of Freund's complete adjuvant for the first injection and incomplete adjuvant for further injections. Blood was collected at 7th day after the last injection and centrifuged at 6,000 rpm for 20 min. The supernatant serum was further purified by precipitation in 40% ammonium sulphate and then purified by protein A affinity chromatography method.

Western Blot Analysis

Purified AlinOBP1 was separated on 15% SDS-PAGE and then transferred to a PolyVinylidene Fluoride (PVDF, Millipore, Carrigtwohill, Ireland) membrane. The membrane was blocked with 5% dry skimmed milk (BD Biosciences, San Jose, CA) in phosphate-buffered saline containing 0.1% Tween-20 (PBST) for 2 h at room temperature and washed three times with PBST (10 min each time). The blocked membrane was then incubated with the purified rabbit anti-AlinOBP1 antiserum (1:10 000 v/v) for 1 h at room temperature and washed with PBST. Subsequently, the membrane was incubated with anti-rabbit IgG horseradish peroxidase (HRP) conjugate and HRP-streptavidin complex (Promega , Madison, WI). After repeated washing, the membrane was incubated and visualized with Enhanced Chemiluminescence detection regents (GE Healthcare Biosciences, Uppsala, Sweden).

Fluorescence Binding Assay

Most of the 114 chemicals used in this study were purchased from Sigma-Aldrich (St Louis, MO). (purity >95%), including 19 aliphatic alcohols, 14 aldehydes, 14 ketones, 17 esters, 1 heterocyclic compounds, 14 aromatic compounds, 22 terpenoids and 13 alkanes (Table 3).

Fluorescence binding assays were performed on the fluorescence spectrophotometer F-96 (Shanghai Lengguang Technology Co., Ltd. Shanghai, China) in a quartz cuvette with 1 cm light path. Both of the slit widths for excitation and emission were 10 nm. The fluorescent probe 1-NPN was dissolved in methanol to 1 mM stock solution. All chemicals used in this study were dissolved in HPLC purity grade methanol.

To measure the affinity of 1-NPN to AlinOBP1, a 2 μM solution of AlinOBP1 in 50 mM Tris-HCl, PH 7.4, was titrated with aliquots of 1 mM 1-NPN stock solution to final concentrations of 2–22 μM. The AlinOBP1/1-NPN complex was excited at 337 nm and emission spectra were recorded between 390 and 500 nm. The affinities of chemicals were measured by competitive binding assay, using 1-NPN as the fluorescent reporter at 2 μM concentration and each chemical with concentration from 2–16 μM.

For determining binding constants, the fluorescence intensity values at the maximum fluorescence emission were plotted against free ligand concentrations. Bound ligand was evaluated from the values of fluorescence intensity assuming the protein was 100% active, with a stoichiometry of 1:1 (protein:ligand) at saturation. The curves were linearized using Scatchard Plot. Dissociation constants of the competitors were calculated from the corresponding IC_{50} values, using the equation: $K_i = [IC_{50}]/(1 + [1-NPN]/K_{1-NPN})$, where [1−NPN] is the free concentration of 1−NPN and K_{1-NPN} is the dissociation constant of the 1−NPN.

3D Structural Modeling

The amino acid sequence of AlinOBP1 was submitted to the FUGUE server (http://tardis.nibio.go.jp/fugue/prfsearch.html) to find structural homologs. With identified structural template and the corresponding sequence alignment, several 3D models were constructed by using the Modeler module in Discovery Studio 2.0 (Accelrys Software Inc. San Diego, CA). The terminal unaligned residues were cut, and the loop regions were refined. The Profiles-3D method was used to evaluate the fitness between the sequence and the established 3D models, and the model with the highest score of Profiles-3D was finally retained.

Immunocytochemistry

Antennae were excised from adult *A. lineolatus* and chemically fixed by immersion in a mixture of paraformaldehyde (4%) and glutaraldehyde (2%) in 0.1 M PBS (pH = 7.4), dehydrated in an ethanol series and then embedded in LR White resin (Taab, Aldermaston, Berks, UK). Ultrathin sections (60–80 nm) were treated with primary antisera (anti-AlinOBP1) diluted at 1:5,000–1:15,000. The secondary antibody was anti-rabbit IgG conjugated with 10 nm colloidal gold granules (Sigma, St. Louis, MO) at a dilution of 1:20. Optional silver intensification (Danscher, 1981) was used to enlarge the size of the gold granules to 30–40 nm. Sections were stained with 2% uranyl acetate to increase the contrast in transmission electron microscopy (HITACHIH-7500). Labeling intensities were observed in 3 male and 3 female antennae for about 150 sensilla in each sex.

RESULTS

cDNA Sequence Analysis

The *AlinOBP1* EST from the antennal cDNA library contains an open reading frame of 438 base pairs. The 3′ end of the *AlinOBP1* EST contains polyadenylation signals typical for eukaryotes and the AATAAA sequence is located 20 bases upstream from GCA at the 5′ end which leads into a poly(A) stretch (Fig. 1). The 5′ end of *AlinOBP1* contains an untranslated sequence of 84 bases before the initial codon ATG. Therefore, *AlinOBP1* EST appears to contain the complete coding region. The predicted amino acid sequence of *AllinOBP1* CDS has the typical six-cysteine signature of insect OBPs (Pelosi, 1998) with a signal peptide of 18 amino acid residues at the N terminus (Fig. 2).

Spatial and Temporal Expression Patterns of AlinOBP1

To quantify the expression level of *AlinOBP1* transcripts in different tissues and developmental stages, we conducted a real-time PCR with the comparative $2^{-\Delta\Delta Ct}$ method (Livak and Schmittgen, 2001). The results indicated that *AlinOBP1* was predominantly expressed in adult antennae, about 2,000-fold higher than in other tissues, and 1.91 times higher in male antennae than in female antennae (Table 2). *AlinOBP1* was expressed throughout all developmental stages with the highest level (47.46%) in adult, which was 8.5, 5.5, 5.2, 4.7, 2.5 times higher than in first to five nymph stage, respectively (Table 2).

Fluorescence Binding Assays

To examine the odorant binding of AlinOBP1 we expressed and purified recombinant AlinOBP1 (Fig. 3). The fluorescence displacement assay was performed using a fluorescence probe 1-NPN. The dissociation constant of the AlinOBP1/1-NPN complex was calculated as 9.09 μM with Scatchard Plot (Fig. 4), which was used to calculate the dissociation constants (K_i) of ligands for the displacement of 1-NPN.

Most of the 19 alcohols tested failed to displace 1-NPN from the AlinOBP1/1-NPN complex at concentrations up to 50 μM. Only one compound (2-ethyl-1-hexanol) showed a good affinity to AlinOBP1 with the dissociation constant (K_i) of 6.76 μM

```
1   CCA TTA CGG CCG GGG GAG ACA CTA GCA ATT TTA CAT CGT CCA TGG TAG ATC ACT GGT GCG
61  CTT CAA GAA TCC ACA AGC GTT ATC ATG AAC TCA CTC ATT CCC GTG TTG TTG GTG GTT TGC
                                    M   N   S   L   I   P   V   L   L   V   V   C
121 GCT GCT GCG ACG AGG GCA GAC GAA CAA ACC AAC GCC ATG GTA GCC AAA GCC TTC AAC AAA
      A   A   A   T   R   A   D   E   Q   T   N   A   M   V   A   K   A   F   N   K
181 TGC CGG GAG GAA TTT CCC ATC AGT GAC GAT GAA ATT GGT GGA GTG AAG GAA AAG ACG ACG
      C   R   E   E   F   P   I   S   D   D   E   I   G   G   V   K   E   K   T   T
241 ATT CCA GAG TCT CAT AAT GCT AAA TGT CTC ATG GCC TGC ATG TTG CGA GAA GGC AAA ATG
      I   P   E   S   H   N   A   K   C   L   M   A   C   M   L   R   E   G   K   M
301 TTG AGA GAT GGA AAA TAC GAA AAG GAA AAC GCT CTT ATA ATG GCT GAT GTA CTG AAC AAG
      L   R   D   G   K   Y   E   K   E   N   A   L   I   M   A   D   V   L   N   K
361 GAT GAT CCT GCC ACT GCT GAT AAA GCA AAA CAG CTT GTA GAA ACA TGT GCA GGC AAA GTT
      D   D   P   A   T   A   D   K   A   K   Q   L   V   E   T   C   A   G   K   V
421 GGG ACA GAT GCA GGT GGG GAC GAA TGC GAG TTT GCT TAC AAA ATG GCT GTG TGC GCT GCG
      G   T   D   A   G   G   D   E   C   E   F   A   Y   K   M   A   V   C   A   A
481 GAA GAA GCA AAG AAG CTT GGA GTG CGT CCT CCA GAC TTC TAA GTA CCA AAA TTT CAA TTG
      E   E   A   K   K   L   G   V   R   P   P   D   F   *
541 TAT TGA TAC ACC ACC ATC GAC TTC GCA CAC CAA ATT TCA GGC ATT CCT CGT CTC TTG ATC
601 CCA CCA AAG TCA TCA TAT TAC CAT AAC GTG AAT TTA AGA CCT TTC ATT TCT TAT AAT TAA
661 GAC TTT AAT ACA TAT TAT GTA AAT CTG GTG GTA ATT GCT GGG TTC ACG AAG CAA TAA AAC
721 TCC TAC AAT TTA CGT ATT GCA AAA AAA AAA AAA AAA AAA AAA AAA AA
```

Figure 1. cDNA and derived amino acid sequences of AlinOBP1. The N-terminal signal peptide sequence and the polyadenylation signal AATAAA are underlined. The stop codon is indicated with an asterisk. Six conserved cysteines are showed with black boxes.

(Fig. 5A). (*Z*)-3-hexen-1-ol and hexanol showed medium binding affinity with K_i of 16.97 and 14.39 μM, receptively.

Three volatiles (octanal, nonanal and decanal) of cotton plants (Yu et al., 2007) in 14 aliphatic aldehydes tested effectively displaced 1-NPN with K_i of 6.91, 7.73 and 5.75 μM, respectively (Fig. 5B). (E)-2-hexenal, another volatile released by the cotton when the plant suffered mechanical injuries (Yu et al., 2007) only showed week binding affinity to AlinOBP1 with K_i of 23.84 μM.

Among the 14 ketones, two cotton volatiles (2-hexanone and 3-hexanone) (Yu et al., 2007) showed week binding to AlinOBP1 with K_i of 25.71 and 13.64 μM, respectively (Fig. 5C).

In 17 aliphatic esters tested, two main potential pheromone components (ethyl butyrate, trans-2-hexenyl butyrate) of most plant bugs (Gueldner and Parrott, 1978; Aldrich, 1988; Millar, 2005) showed significant binding affinities to AlinOBP1 with K_i of 2.30 and 4.11 μM, respectively (Fig. 5D). Hexyl butanoate, a putative pheromone in

Figure 2. Alignment of AlinOBP1 with other insect OBPs. Full-length amino acid sequences of AlinOBPs are aligned by ClustalX 1.83 and edited using GeneDoc. Signal peptides are underlined. Six conserved cysteines are labeled in red. The other insect species are: *Drosophila melanogaster* (Dmel), *Tribolium castaneum* (Tcas), *Bombyx mori* (Bmor), *Apis mellifera* (Amel), *Euschistus heros* (Eher), *Acyrthosiphon pisum* (Apis), *Lygus lineolaris* (Llin). GenBank accession numbers for the 8 OBPs are: AlinOBP1, GQ477022; DmelOBP76a, NM_079438; TcasOBP1, XM_970591; BmorGOBP1, NM_001044031; AmelASP1, AF393494; EherOBP1, HM347779; ApisOBP8, NM_001160062; LlinAP, AF091118.

Table 2. Relative Quantification Data of AlinOBP1 in Different Tissues and Developmental Stages. (A) Relative Quantification Data of AlinOBP1 in Different Tissues and (B) Relative Quantification Data of AlinOBP1 During Developmental Stages

Tissues	*OBP1* C_T	β-*actin* C_T	ΔC_T	$\Delta\Delta C_T$	$2^{-\Delta\Delta Ct}$ *(range)*
(A)					
Male-antennae	21.31 ± 0.10	23.48 ± 0.03	−2.17 ± 0.11	0.00 ± 0.11	1.00 (0.92658–1.07923)
Female-antennae	23.35 ± 0.12	24.59 ± 0.01	−1.24 ± 0.12	0.93 ± 0.12	0.524858 (0.48297–0.57038)
Heads	30.48 ± 0.08	22.33 ± 0.05	8.15 ± 0.05	10.32 ± 0.05	0.00078 (0.00076–0.00081)
Thoraxes	30.28 ± .011	21.61 ± 0.02	8.69 ± 0.09	10.85 ± 0.09	0.00054 (0.00051–0.00058)
Abdomens	30.65 ± 0.11	21.73 ± 0.05	8.93 ± 0.15	11.10 ± 0.15	0.00045 (0.00041–0.00051)
Legs	29.94 ± 0.03	21.16 ± 0.07	8.78 ± 0.06	10.95 ± 0.06	0.00051 (0.00048–0.00053)
Wings	30.78 ± 0.19	21.32 ± 0.02	9.46 ± 0.20	11.63 ± 0.20	0.00032 (0.00027–0.00036)
(B)					
1 instar	28.01 ± 0.06	20.00 ± 0.05	8.01 ± 0.09	0.00 ± 0.09	1 (0.94–1.06)
2 instar	26.67 ± 0.09	19.29 ± 0.11	7.38 ± 0.19	−0.62 ± 0.19	1.54 (1.35–1.77)
3 instar	28.04 ± 0.09	20.74 ± 0.12	7.30 ± 0.16	−0.71 ± 0.16	1.64 (1.46–1.83)
4 instar	28.59 ± 0.09	21.46 ± 0.07	7.14 ± 0.13	−0.87 ± 0.13	1.83 (1.67–2.00)
5 instar	27.19 ± 0.09	20.95 ± 0.04	6.24 ± 0.11	−1.77 ± 0.11	3.41 (3.16–3.68)
Adult	27.45 ± 0.07	22.53 ± 0.09	4.92 ± 0.17	−3.09 ± 0.17	8.51 (7.57–9.58)

OBP1 C_T = Ave.*OBP1* C_T, β-*actin* C_T = Ave. β-*actin* C_T, ΔC_T = Ave.*OBP1* C_T- Ave. β-*actin* C_T, $\Delta\Delta C_T$ = Ave.$\Delta C_{T,\ X}$ - Ave. $\Delta C_{T,\ \text{Male-antennae}}$, X represents different tissues. $2^{-\Delta\Delta Ct}$ means normalized *AlinOBP1* amount relative to male antennae. *OBP1* C_T = Ave.*OBP1* C_T, β-*actin* C_T = Ave. β-*actin* C_T, ΔC_T = Ave.*OBP1* C_T- Ave. β-*actin* C_T, $\Delta\Delta C_T$ = Ave.$\Delta C_{T,\ X}$ - Ave. $\Delta C_{T,\ 1\ \text{instar}}$, X represents different stages. $2^{-\Delta\Delta Ct}$ means normalized *AlinOBP1* amount relative to 1 instar.

the *Lygus lineolaris* (Hemiptera: Miridae) (Wardle et al., 2003), showed a week binding affinity to AlinOBP1 with K_i of 16.16 μM (Fig. 5D). Another two pheromone components (butyl butanoate and hexyl hexanoate) of related plant bugs (Aldrich, 1988; Millar, 2005), however, had low affinities to AlinOBP1 with K_d of 44.06 and 33.93 μM, respectively (Fig. 5D). (*Z*)-3-hexenyl acetate, a chemical identified as an

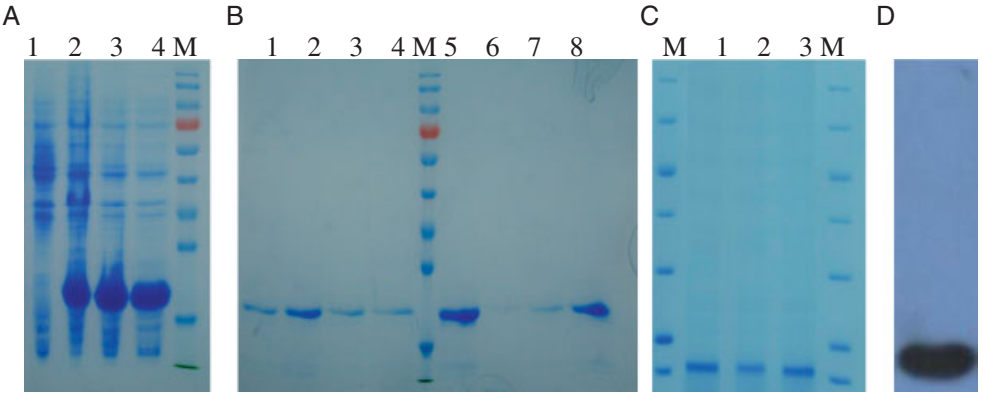

Figure 3. (**A**) SDS-PAGE analysis of the expressed product of PET/AlinOBP1. (**B**) Purified AlinOBP1 protein with his-tag. (**C**) Purified AlinOBP1 prorein without his-tag. (**D**) Western blot analysis of purified AlinOBP1. (A) lane 1: PET/AlinOBP1 transformed BL21(DE3), noninduced; Lane 2: PET/AlinOBP1 transformed BL21(DE3), induced; Lane 3: The pellet of PET/AlinOBP1; Lane 4: The supernatant of PET/AlinOBP1; M: Protein molecular weight marker, from the top: 170, 130, 95, 72, 55, 43, 34, 26, 17, 10 KDa. (B) lanes 1–4: Purified AlinOBP1 was eluted with 300 mM imidazole; lanes 5–8: Purified AlinOBP1 was eluted with 400 mM imidazole; M: Protein molecular weight marker, from the top: 170, 130, 95, 72, 55, 43, 34, 26, 17, 10 KDa. (C) lane 1–3: Repurified AlinOBP1 protein after recombinant enterokinase cleavaged the his-tag. M: Protein molecular weight marker, from the top: 116.0, 66.2, 45.0, 35.0, 25.0, 18.4, 14.4 KDa. (D) Western Blot analysis of the purified AlinOBP1 using polyclonal rabbit antiserum.

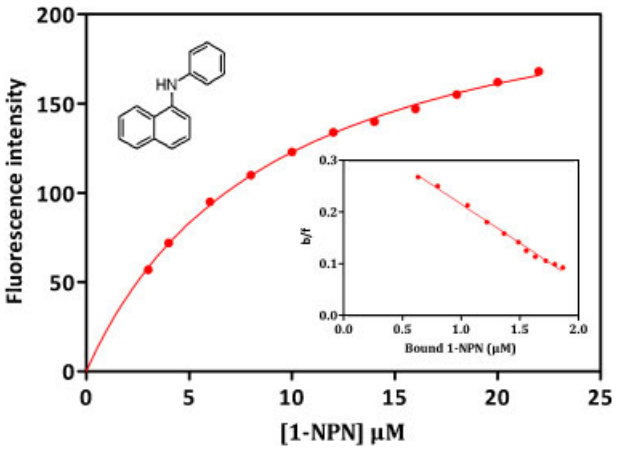

Figure 4. Binding of 1-NPN to AlinOBP1. Protein was 2 μM in Tris buffer, pH 7.4. Aliquots of a 1 mM methanol solution of 1-NPN were added to the protein to final concentrations of 2, 4, 6, 8, 10, 12, 14, 16, 18, 20, 22 μM, and the emission spectra were recorded between 390 and 500 nm. The binding curve and the relative Scathard plot indicate a binding constant of 9.09 μM.

efficient attractant to the cotton mirids in the field (Drukker et al., 2000; James, 2003), showed a week binding affinity with AlinOBP1 (K_i = 19.26 μM).

In the 22 aliphatic terpenoids and 14 aromatic compounds, benzaldehyde, a volatile released from cotton plants (Yu et al., 2007) was able to bind AlinOBP1 with K_i of 13.64 μM (Fig. 5E), whereas other two volatiles (β-caryophyllene and myrcene) from cotton plants (Yu et al., 2007) exhibited a high binding affinity to AlinOBP1 with K_i of 2.84 and 6.49 μM, respectively (Fig. 5F). In particular, β-ionone was observed to have

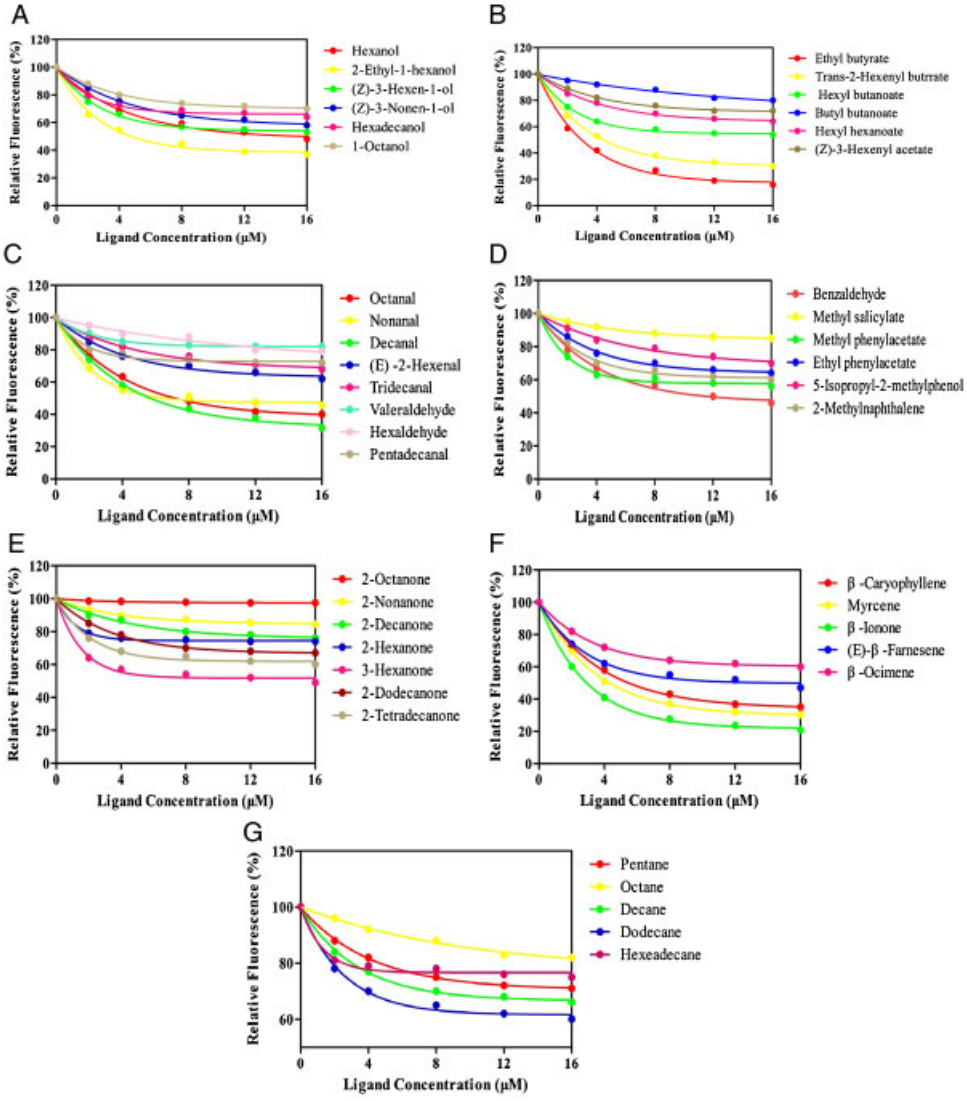

Figure 5. Competitive binding curves of selected ligands to AlinOBP1. A mixture of the protein and 1-NPN in Tris buffer, pH = 7.4, both at the concentration of 2 μM, with titrated with aliquots of 1 mM methanol solutions of the ligands to final concentrations of 2–16 μM. Fluorescence values were tested as percent of the values in the absence of competitor. Data are means of three independent experiments. (**A**) Binding curves of selected Aliphatic alcohols. (**B**) Binding curves of selected Aliphatic aldehydes. (**C**) Binding curves of selected Aliphatic ketones. (**D**) Binding curves of selected Aliphatic esters. (**E**) Binding curves of selected Aromatic compounds. (**F**) Binding curves of selected Aliphatic terpenoids. (**G**) Binding curves of selected Aliphatic alkanes.

the best binding affinity among all 114 chemicals tested with K_i of 1.88 μM (Fig. 5F). Moreover, (*E*)-β-farnesene, identified as alarm pheromone in most aphid species (Edwards et al., 1973), showed a medium binding affinity to AlinOBP1 with K_i of 11.12 μM.

In the 13 aliphatic alkanes tested, several long chain chemicals (C8–C16) were identified as volatiles from cotton or recognized as sex pheromones in some species to mediate communication between individuals in some social insects (Turillazzi et al.,

2000). However, few of these potential ligands were able to displace 1-NPN from the complex. Most of the $IC_{50} > 50\,\mu M$ (Fig. 5G).

Structural Model of AlinOBP1

AlinOBP1 shared a low sequence similarity to any insect OBPs of known structures. To predict 3D structure of AlinOBP1, the fold recognition method FUGUE (Shi et al., 2001) was employed to identify structural homologs. The *B. mori* pheromone binding protein 1 BmorPBP1 with bound bombykol (PDB code: 1dqe) (Sandler et al., 2000) was finally chosen as template. Although the sequence identity between AlinOBP1 and BmorPBP1 is only 16.8%, the resulting FUGUE *Z*-score is 16.71, implying a 99% confidence level (generally FUGUE *Z*-score ≥ 6.0 mean $< 1\%$ false-positive rate). Using the sequence alignment (Fig. 6A) generated by FUGUE, the predicted 3D structural model of AlinOBP1 was established with Modeler (Šali and Blundell, 1993), which matches AlinOBP1 from amino acid residue 1–127. The verify score of the final AlinOBP1 model checked by Profiles-3D (Lüthy et al., 1992) is 43.35, which is much higher than expected score (25.83), implying that the overall stereochemical quality of the predicted AlinOBP1 structure is generally reliable.

The predicted 3D model of AlinOBP1 consists of six α-helices located between residues 2–19 (α1), 24–28 (α2), 39–52 (α3), 63–72 (α4), 77–94 (α5) and 102–120 (α6) (Fig. 6B). Three pairs of disulfide bridges connect Cys15 in α1 with Cys47 in α3, Cys43 in α3 with Cys103 in α6, Cys90 in α5 with Cys112 in α6, which could be important for maintaining the stability of AlinOBP1 structure (Fig. 6B). The 3D model of AlinOBP1 predicts a large binding pocket. Based on the crystal structure of BmorPBP1 we roughly assigned those residues at same alignment positions of the binding pocket residues of BmorPBP1 as the potential binding residues of AlinOBP1. Most of the proposed binding residues in AlinOBP1 are also hydrophobic, including Val8, Val29, Met45, Leu49, Met54, Leu55, Ala69, Ala83, Val87, Ala91, Ala106, Met109, Ala110 and Ala113 (Fig. 6B). However, some hydrophilic residues (Asp1, Thr4, Asn5, Arg30, Glu61 and Lys84) are also present in the binding pocket (Fig. 6B), which may be responsible for the formation of hydrogen bonds with the functional groups of some ligands.

Cellular Localization of AlinOBP1

The polyclonal antiserum against AlinOBP1 was used for the localization of AlinOBP1 in antennal sensilla of male *A. lineolatus*. In sections of different chemosensory sensilla, gold particles only labeled the sensilla trichodea and sensilla basiconica. The sensillum lymph in the hair lumen and the cavity below the hair base were heavily labeled (Fig. 7A and B), whereas neither the dendritic cytoplasm nor the cuticle of the hair wall was labeled. No labeling was observed with the sensilla chaetica (Fig. 7C and D). The immunolocalization of AlinOBP1 in antennal sensilla of female *A. lineolatus* was similar as in the male antennae (data not shown).

DISCUSSION

The expression profiles of *AlinOBP1* transcript showed that the gene mainly expressed in the antennae as well as in each developmental stage, suggested an important role of AlinOBP1 in olfaction. The expression of the protein at a high level in the sensilla trichodea and sensilla basiconica of the antennae further supports such role of

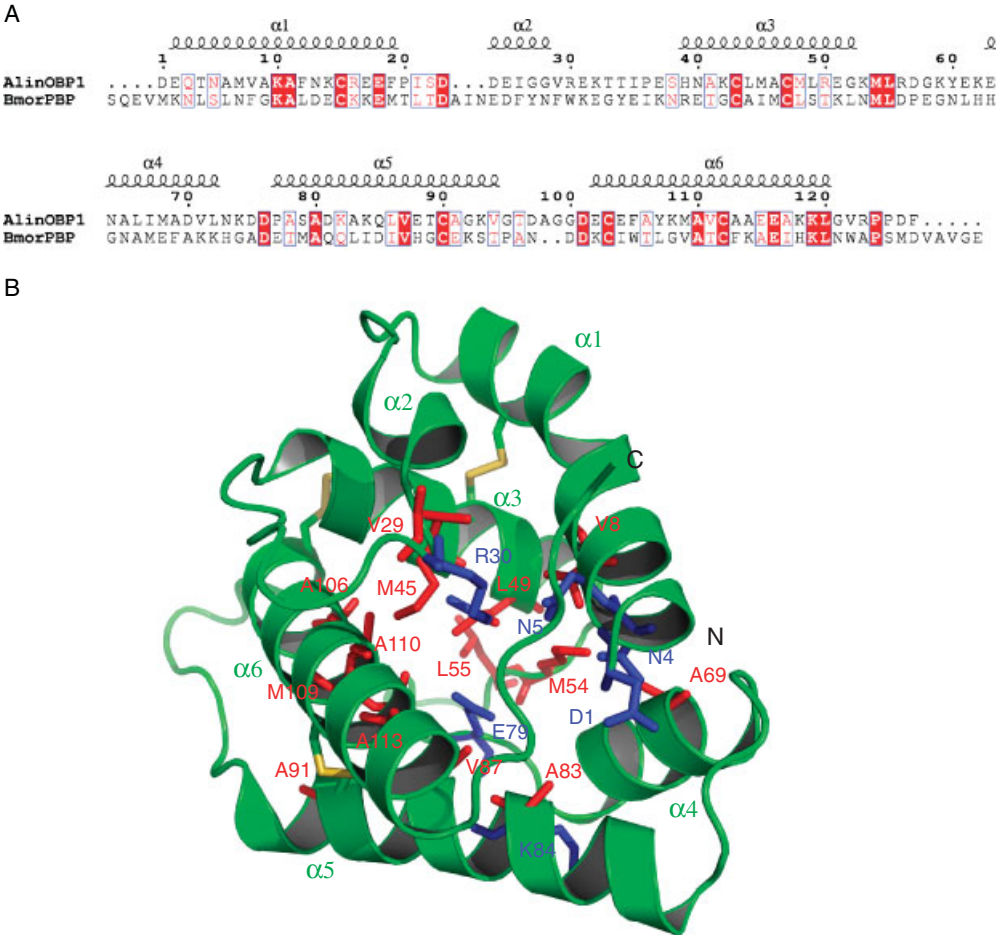

Figure 6. Structural modeling of AlinOBP1. (**A**) Sequence alignment between AlinOBP1 and BmorPBP generated from FUGUE. The secondary structure elements for AlinOBP1 are shown on the top of the sequences. α-helices are displayed as squiggles. Strictly identical residues are highlighted in white letters with a red background. Residues with similar physico-chemical properties are shown in red letters. Alignment positions are framed in blue if the corresponding residues are identical or similar. (**B**) Cartoon representation of AlinOBP1. Helices and two termini are labeled. Residues surrounding the binding pocket are shown as stick, where hydrophobic and hydrophilic residues are colored red and blue, respectively. Disulfide bridges are colored yellow.

AlinOBP1 in the plant bug *A. lineolatus*. It is possible that AlinOBP1 functions as a carrier to transport semiochemicals to the chemosensory receptors both in adults and larvae.

Our fluorescent binding results strongly support a selective binding of AlinOBP1. We did not detect any binding of AlinOBP1 to 13 aliphatic alkanes, and very low binding to 19 alcohols and 14 aldehydes with K_i larger than 5 μM. Three of 14 aldehydes gave a medium binding affinity to AlinOBP1 with K_i about 7 μM. AlinOBP1 showed relative high affinity with K_i less than 5 μM to ethyl butyrate and trans-2-hexenylbutyrate out of 17 esters, β-ionone and β-caryophyllene out of 22 terpenoids. The pheromone components of *A. lineolatus* have not been identified. However, ethyl butyrate and trans-2-hexenyl butyrate have been reported as two major potential pheromone components of most plant bugs (Gueldner and Parrott, 1978; Aldrich, 1988; Millar, 2005). Interestingly, AlinOBP1 showed very low affinity to other

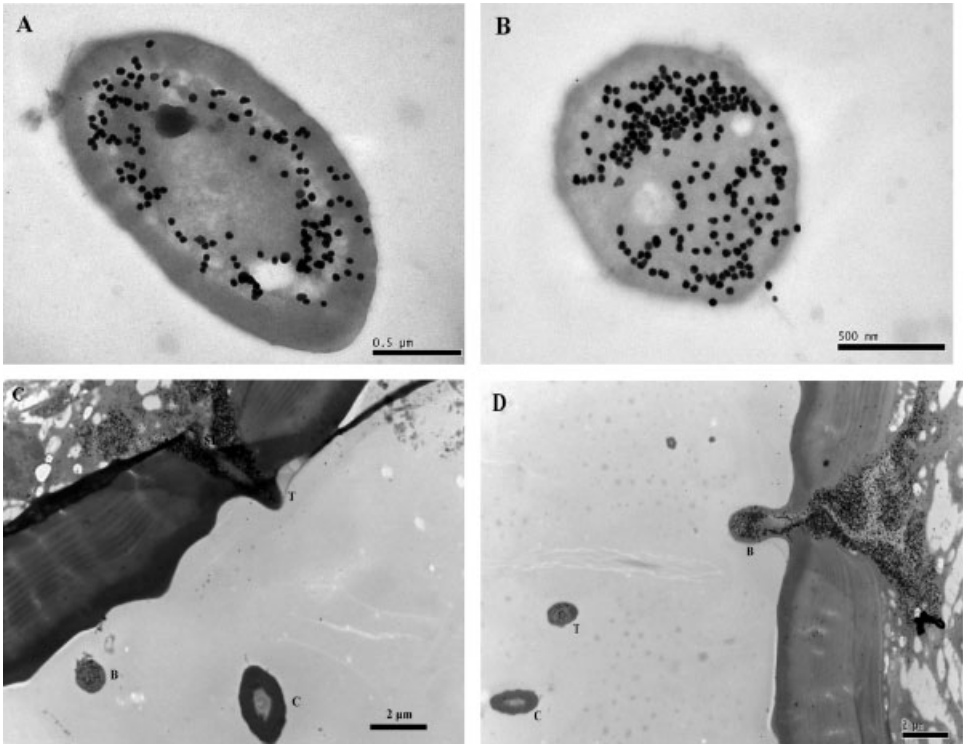

Figure 7. (**A–D**) Immunocytochemical localization of AlinOBP1 in the antennal sensilla of male *A. lineolatus*. A and C, Oblique and longitudinal sections of the sensilla trichodea (T). In both sections, the sensillum lymph (SL) of the pheromone-sensitive sensilla trichodea was strongly labeled by anti-AlinOBP1. In the below part of section C, also see sensilla basiconica (B) was heavily labeled, whereas the sensilla chaetica (C) was never labeled. B, D: Cross and longitudinal sections of the sensilla basiconica. The sensillum lymph in the hair lumen and in the cavity below the hair base is heavily labeled by anti-AlinOBP1, Whereas in the below left part in section D, a heavily labeled sensilla basiconica and a nonlabeled sensilla chaetica was also visible. The few grains found in over the cuticle and the dendrites represent nonspecific background. Dilution of primary antibody was 1:5,000 in A, C and 1:10000 in B, D. Secondary antibody was anti-rabbit IgG conjugated with 10 nm colloidal gold granules at a dilution of 1:20.

pheromone components such as hexyl butanoate and hexanol of the *L. lineolaris* (Hemiptera: Miridae) (Wardle et al., 2003), and butyl butanoate and hexyl hexanoate of related plant bugs (Aldrich, 1988; Millar, 2005) (Fig. 5D).

AlinOBP1 had a very high binding affinity to β-caryophyllene and β-ionone, the most abundant plant volatiles in essential oils with K_i less than 3 μM. However, (*Z*)-3-hexenyl acetate, a chemical identified as an efficient attractant to the cotton mirids in field condition (Drukker et al., 2000; James, 2003) showed a week binding affinity to AlinOBP1 ($K_i = 19.26$ μM). AlinOBP1 binds to 2-ethyl-1-hexanol and myrcene with medium affinity with K_i of 6.76 and 6.49 μM, respectively. All these chemicals were identified as volatiles released from cotton plants under natural conditions or suffered mechanical injuries or/and herbivore-induced (Yu et al., 2007). The binding experiments further demonstrate the possible involvement of AlinOBP1 in the olfactory perception of *A. lineolatus*.

It has been reported in similar binding experiments of locust OBP1 that medium- and long-chain (C11–C17) aliphatic alcohols, such as pentadecanol (C15), hexadecanol

Table 3. Binding affinities of 114 chemical compounds to AlinOBP1

Ligands	K_i (μM)	*Ligands*	K_i (μM)	*Ligands*	K_i (μM)
Aliphatic alcohols		*Aliphatic aldehydes*		2-Octanone (C8)	u.d.
3-Methyl-1-butanol (C5)	u.d.[a]	Valeraldehyde (C5)	45.49 ± 1.32	2-Nonanone (C9)	u.d.
1-Pentanol (C5)	u.d.	(E) -2-Hexenal (C6)	23.84 ± 0.90	2-Decanone (C10)	u.d.
(Z)-3-Hexen-1-ol (C6)	16.97 ± 1.73	Hexaldehyde (C6)	46.19 ± 1.51	2-Undecanone (C11)	u.d.
Hexanol (C6)	14.39 ± 1.10	Heptanal (C7)	u.d.	2-Dodecanone (C12)	38.58 ± 1.56
2-Hexanol (C6)	40.59 ± 1.82	Octanal (C8)	6.91 ± 0.13	2-Tridecanone (C13)	u.d.
1-Heptanol (C7)	u.d.	Nonanal (C9)	7.73 ± 0.23	2-Tetradecanone (C14)	36.76 ± 1.78
2-Ethyl-1-hexanol (C8)	6.76 ± 0.84	Decanal (C10)	5.75 ± 0.17	2-pentadecanone (C15)	u.d.
1-Octanol (C8)	26.03 ± 1.87	Undecylic aldehyde (C11)	u.d.	2-Hexadecanone (C16)	u.d.
2-Octanol (C8)	u.d.	Dodecanal (C12)	u.d.	2-Heptadecanone (C17)	u.d.
Nonanol (C9)	40.18 ± 0.93	Tridecanal (C13)	39.96 ± 1.09	*Aliphatic esters*	
(Z)-3-Nonen-1-ol (C9)	22.73 ± 0.24	Tetradecanal (C14)	u.d.	Ethyl butyrate (C6)	2.30 ± 0.18
1-Decanol (C10)	34.91 ± 1.37	Pentadecanal (C15)	44.97 ± 1.77	Butyl acetate (C6)	u.d.
Undecanol (C11)	u.d.	Palmitic aldehyde (C16)	u.d.	3-Methylbutanoic acid etnyl ester (C7)	u.d.
Dodecanol (C12)	u.d.	Heptadecyl aldehyde (C17)	u.d.	2-Propenoic acid butyl ester (C7)	40.25 ± 1.73
Tridecanol (C13)	38.53 ± 1.84	*Aliphatic ketones*		Amyl acetate (C7)	35.92 ± 0.92
Tetradecanol (C14)	43.86 ± 1.18	2-Hexanone (C6)	25.71 ± 0.81	Ethyl 2-methylbutyrate (C7)	u.d.
Pentadecanol (C15)	u.d.	3-Hexanone (C6)	13.64 ± 0.10	Butyl propanoate (C7)	u.d.
Hexadecanol (C16)	34.16 ± 0.89	2-Heptanone (C7)	u.d.	2-Methylbutyl acetate (C7)	u.d.
Heptadecanol (C17)	u.d.	6-Methyl-5-hepten-2-one (C8)	u.d.	Butyl butanoate (C8)	44.06 ± 1.56

(Z)-3-Hexenyl acetate (C8)	19.26±0.68	Naphthalene (C10)	u.d.	β-Ionone (C13)	1.88±0.10
Ethyl heptanoate (C9)	u.d.	2-Methylnaphthalene (C11)	27.91±1.10	Nerolidol (C15)	u.d.
1-Hexyl butanoate (C10)	16.16±0.44	*Heterocyclic compound*		Farnesol (C15)	u.d.
Ethyl caprylate (C10)	u.d.	2,3-Benzopyrrole (C8)	25.41±1.23	β-Caryophyllene (C15)	2.84±0.25
Trans-2-Hexenyl butyrate (C10)	4.11±0.14	*Aliphatic terpenoids*		Humulene (C15)	u.d.
Nonyl acetate (C11)	u.d.	Limonene (C10)	u.d.	(E)-β-Farnesene (C15)	11.12±0.33
Hexyl hexanoate (C12)	33.93±1.01	3-Carene (C10)	u.d.	*Aliphatic alkanes*	
(2E)-3,7-Dimethyl-2,6-octadienyl butyrate (C14)	u.d.	α-Pinene (C10)	21.15±0.64	Pentane (C5)	36.17±1.59
Aromatic compounds		β-Pinene (C10)	u.d.	Hexane (C6)	u.d.
Benzaldehyde (C7)	13.64±0.19	Citral (C10)	u.d.	Heptane (C7)	u.d.
Benzoic acid (C7)	33.76±1.15	βOcimene (C10)	18.19±0.61	Octane (C8)	41.94±1.64
Ethylbenzene (C8)	u.d.	αOcimene (C10)	31.12±1.28	Nonane (C9)	u.d.
Acetophenone (C8)	u.d.	Linalool (C10)	u.d.	Decane (C10)	33.57±1.41
Methyl salicylate (C8)	41.38±1.60	Geraniol (C10)	u.d.	Undecane (C11)	u.d.
1,3-Dimethylbenzene (C8)	u.d.	β-Citronellol (C10)	u.d.	Dodecane (C12)	25.55±1.16
Methyl phenylacetate (C9)	28.54±0.80	(−)-Carveol (C10)	25.51±1.21	Tridecane (C13)	u.d.
4-Ethyl-benzaldehyde (C9)	u.d.	α-Phellandrene (C10)	u.d.	Tetradecane (C14)	u.d.
3,4-Dimethyl-benzaldehyde (C9)	u.d.	Isoborneol (C10)	u.d.	Pentadecane (C15)	u.d.
2,3-Dimethylbenzoic acid (C9)	u.d.	Camphorquinone (C10)	u.d.	Hexeadecane (C16)	37.28±1.55
Ethyl phenylacetate (C10)	28.30±0.64	Myrcene (C10)	6.49±0.19	Heptadecane (C17)	u.d.
5-Isopropyl-2-methylphenol (C10)	32.21±1.55	α-Terpinene (C10)	–		

[a]u.d.indicates that the dissociation constants were unable to be calculated because the half-maximal inhibition was >50 μM of odorant concentrations.

(C16), heptadecanol (C17), were potential competitors that could displace 1-NPN more effectively than that with short-chain (C6–C10) ligands (Jiang et al., 2009). However, in our case, these C11–C17 aliphatic alcohols completely failed to bind to AlinOBP1 or showed very weak binding affinity, even at the concentrations of 50 μM (Table 3). These results suggested the differences in the binding of aliphatic alcohols by different OBPs from different species, and it also demonstrated that there is no linear relationship between the carbon number of alcohols and their binding affinities for AlinOBP1.

Some ligands which had the same molecular formula and function group but differed in conformation, such as hexanol/2-hexanol, 1-octanol/2-octanol, 2-hexanone/3-hexanone, α-ocimene/β-ocimene, were used to test the binding affinity of AlinOBP1. The dissociation constants of these isomers to AlinOBP1 were significantly different. It indicated that the binding affinity of OBPs was affected by the conformation changes of ligands, consistent with previous studies (Honson et al., 2005). Similarly, the binding differences were also observed between aldehydes and ketones. We found octanal, nonanal and decannal had higher binding abilities ($K_i < 8\,\mu M$) to AlinOBP1 than 2-octanone, 2-nonanone and 2-decanone ($K_i > 50\,\mu M$) (Fig. 5B).

We predicted 3D structure of AlinOBP1 to strengthen our understanding of its ligand-binding ability. In this model, the binding pocket is mainly organized by hydrophobic amino acids, which may be responsible for the hydrophobic interactions with ligands such as β-caryopphyllene. However, some hydrophilic residues are also presented in the binding pocket (Fig. 6B), which could form hydrogen bonds and to enhance the binding to ligands such as β-ionone. Some of the hydrophilic residues locate in the opening of the binding cavity (Jiang et al., 2009) and are likely to be involved in the formation of hydrogen bonds with the functional group of ligands and play a key role in the initial ligand recognition. However, these presumptions need to be confirmed by real 3D structure of AlinOBP1 which can be solved by X-ray diffraction or NMR. The hypothetical function of the hydrophilic amino acids located in the opening of the binding cavity also needs to be identified by site-directed mutagenesis experiments.

ACKNOWLEDGMENTS

This work was supported by the China National "973" Basic Research Program (2007CB109202), the National Natural Science Foundation of China (31071694 and 30871640), and the State High Technology Development Program (2008AA02Z307 to Z.Z.).

LITERATURE CITED

Aldrich JR. 1988. Chemical ecology of the Heteroptera. Annu Rev Entomol 33:211–238.

Ban L, Scaloni A, D'ambrosio C, Zhang L, Yan Y, Pelosi P. 2003. Biochemical characterization and bacterial expression of an odorant-binding protein from *Locusta migratoria*. Cell Mol Life Sci 60:390–400.

Breer H, Raming K, Krieger J. 1994. Signal recognition and transduction in olfactory neurons. Biochim Biophs Acta 1224:277–287.

Calvello M, Guerra N, Brandazza A, D'Ambrosio C, Scaloni A, Dani FR, Turillazzi S, Pelosi P. 2003. Soluble proteins of chemical communication in the social wasp *Polistes dominulus*. Cell Mol Life Sci 60:1933–1943.

Danscher G. 1981. Localization of gold in biological tissue. A photochemical method for light and electronmicroscopy. Histochemistry 71:81–88.

Dickens JC, Callahan FE, Wergin WP, Erbe EF. 1995. Olfaction in a hemimetabolous insect: antennal-specific protein in adult *Lygus lineolaris* (Heteroptera: Miridae). J Insect Physiol 41:857–867.

Drukker B, Bruin J, Sabells M. 2000. Anthocorid predators learn to associate herbivore-induced plant volatiles with presence or absence of prey. Physiol Entomol 25:260–265.

Edwards LJ, Siddall JB, Dunham LL, Uden P, Kislow CJ. 1973. Trans-β-farnesene, alarm pheromone of the green peach aphid, *Myzus perssicae* (Sulzer). Nature 241:126–127.

Field LM, Pickett JA, Wadhams LJ. 2000. Molecular studies in insect olfaction. Insect Mol Biol 9:545–551.

Graham LA, Brewer D, Lajoie G, Davies PL. 2003. Characterization of a subfamily of beetle odorant-binding proteins found in hemolymph. Mol Cell Proteomics 2:541–549.

Greene JK, Turnipseed SG, Sullivan MJ, Herzog GA. 1999. Boll damage by southern green stink bug (Hemiptera: Pentatomidae) and tarnished plant bug (Hemiptera: Miridae) caged on transgenic *Bacillus thuringiensis* cotton. J Ecol Entomol 92:941–944.

Gu SH, Wang SP, Zhang XY, Wu KM, Guo YY, Zhou JJ, Zhang YJ. 2011. Identification and tissue distribution of odorant binding protein genes in the lucerne plant bug *Adelphocoris lineolatus* (Goeze). Insect Biochem Mol Biol 41:254–263.

Gueldner RC, Parrott WL. 1978. Volatile constituents of the tarnished plant bug. Insect Biochem 8:389–391.

He X, Tzotzos G, Woodcock C, Pickett JA, Hooper T, Field LM, Zhou JJ. 2010. Binding of the general odorant binding protein of *Bombyx mori* BmorGOBP2 to the moth sex pheromone components. J Chem Ecol 36:1293–1305.

Honson NS, Gong Y, Plettner E. 2005. Structure and function of insect odorant and pheromone-binding proteins (OBPs and PBPs) and chemosensory-specific proteins (CSPs). Recent Ad Phytochem 39:227–268.

James DG. 2003. Field evaluation of herbivore-induced plant volatiles as attractants for beneficial insects: methyl salicylate and the green lacewing, *Chrysopa nigricornis*. J Chem Ecol 29:1601–1609.

Jiang QY, Wang WX, Zhang ZD, Zhang L. 2009. Binding specificity of locust odorant binding protein and its key binding site for initial recognition of alcohols. Insect Biochem Mol Biol 39:440–447.

Krieger J, Breer H. 1999. Olfactory reception in invertebrates. Science 286:720–728.

Krieger MJ, Ross KG. 2002. Identification of a major gene regulating complex social behavior. Science 295:328–332.

Krieger J, Nickisch-Rosenegk EV, Mameli M, Pelosi P, Breer H. 1996. Binding proteins from the antennae of *Bombyx mori*. Insect Biochem Mol Biol 26:297–307.

Livak KJ, Schmittgen TD. 2001. Analysis of relative gene expression data using real-time quantitative PCR and the $2^{-\Delta\Delta Ct}$ method. Methods 25:402–408.

Lu YH, Wu KM, Jiang YY, Xia B, Li P, Feng HQ, Wyckhuys KAG, Guo YY. 2010. Mirid bug outbreaks in multiple crops correlated with wide-scale adoption of Bt cotton in China. Science 328:1151–1154.

Lüthy R, Bowie JU, Eisenberg D. 1992. Assessment of protein models with three-dimensional profiles. Nature 356:83–85.

Millar JG. 2005. Pheromones of true bugs. Top Curr Chem 240:37–84.

Pelosi P. 1998. Odorant-binding proteins: structural aspects. Ann N Y Acad Sci 855:281–293.

Pelosi P, Zhou JJ, Ban LP, Calvello M. 2006. Soluble proteins in insect chemical communication. Cell Mol Life Sci 63:1658–1676.

Plettner E. 2002. Insect pheromone olfaction: new targets for the design of species-selective pest control agents. Curt Med Chem 9:1075–1085.

Šali A, Blundell TL. 1993. Comparative protein modeling by satisfaction of spatial restraints. J Mol Biol 234:779–815.

Sandler BH, Nikonova L, Leal WS, Clardy J. 2000. Sexual attraction in the silkworm moth: structure of the pheromone-binding-protein-bombykol complex. Chem Biol 7:143–151.

Shi J, Blundell TL, Mizuguchi K. 2001. FUGUE: sequence-structure homology recognition using environment-specific substitution tables and structure-dependent gap penalties. J Mol Biol 310:243–257.

Steinbrecht RA. 1998. Odorant-binding proteins: Expression and function. Ann NY Acad Sci 855:323–332.

Turillazzi S, Sledge MF, Dani FR, Cervo R, Massolo A, Fondelli L. 2000. Social hackers: integration in the host chemical recognition system by a paper wasp social parasite. Naturwissenschaften 87:172–176.

Vogt RG, Riddiford LM. 1981. Pheromone binding and inactivation by moth antennae. Nature 293:161–163.

Vogt RG, Riddiford LM, Prestwich GD. 1985. Kinetic properties of a pheromone-degrading enzyme: the sensillar esterase of *Antheraea polyphemus*. Proc Natl Acad Sci 82:8827–8831.

Vogt RG, Rybczynski R, Lerner MR. 1991. Molecular cloning and sequencing of general-odorant binding proteins GOBP1 and GOBP2 from the tobacco hawk moth *Manduca sexta*: comparisons with other insect OBPs and their signal peptides. J Neurosci 11:2972–2984.

Vogt RG, Miller NE, Litvack R, Fandino RA, Sparks J, Staples J, Friedman R, Dickens JC. 2009. The insect SNMP gene family. Insect Biochem Mol Biol 39:448–456.

Wanner KW, Willis LG, Theilmann DA, Isman MB, Feng Q, Plettner E. 2004. Analysis of the insect *OS-D*-like gene family. J Chem Ecol 30:889–911.

Wardle AR, Borden JH, Pierce HD, Gries R. 2003. Volatile compounds released by disturbed and calm adults of the tarnished plant bug, *Lygus lineolaris*. J Chem Ecol 29:931–944.

Wu K, Li W, Feng H, Guo Y. 2002. Seasonal abundance of the mirids, *Lygus lucorum* and *Adelphocoris* spp. (Hemiptera: Miridae) on Bt cotton in northern China. Crop Prot 21:997–1002.

Xu PX, Zwiebel LJ, Smith DP. 2003. Identification of a distinct family of genes encoding atypical odorant-binding proteins in the malaria vector mosquito, *Anopheles gambiae*. Insect Mol Biol 12:549–560.

Yu HL, Zhang YJ, Pan WL, Guo YY, Gao XW. 2007. Identification of volatiles from field cotton plant under different induction treatments. Chin J Appl Ecol 18:859–864.

Yu F, Zhang S, Zhang L, Pelosi P. 2009. Intriguing similarities between two novel odorant-binding proteins of locusts. Biochem Biophys Res Commun 385:369–374.

Zhang S, Zhang YJ, Su HH, Gao XW, Guo YY. 2009. Identification and expression pattern of putative odorant-binding proteins and chemosensory proteins in antennae of the *Microplitis mediator* (Hymenoptera: Braconidae). Chem Senses 34:503–512.

Zhou JJ. 2010. Odorant-binding proteins in insects. Vitam Horm 83:241–272.

Zhou JJ, Zhang GA, Huang W, Birkett MA, Field LM, Pickett JA, Pelosi P. 2004. Revisiting odorant-binding protein LUSH of *Drosophila melanogaster*: evidence for odour recognition and discrimination. FEBS Lett 558:23–26.

Zhou JJ, Robertson G, He XL, Dufour S, Hooper AM, Pickett JA, Keep NH, Field LM. 2009. Characterisation of *Bombyx mori* odorant-binding proteins reveals that a general odorant-binding protein discriminates between sex pheromone components. J Mol Biol 389:529–545.

Zhou JJ, Field LM, He XL. 2010. Insect odorant-binding proteins: do they offer an alternative pest control strategy? Outlooks on Pest Manage 21:31–34.

Ziegelberger G. 1995. Redox-shift of the pheromone-binding protein in the silkmoth *Antheraea polyphemus*. Eur J Biochem 232:706–711.